Eur. Phys. J. C (2024) 84:1089
https://doi.org/10.1140/epjc/s10052-024-13362-9

THE EUROPEAN PHYSICAL JOURNAL C

Regular Article - Theoretical Physics

Gravitational lensing around a dual-charged stringy black hole in plasma background

Shubham Kala[1,2,a], **Hemwati Nandan**[3,4,b], **Amare Abebe**[4,5,c], **Saswati Roy**[6,d]

[1] Department of Physics, B. D. Government Post Graduate College, Jaiharikhal, Pauri Garhwal, Lansdowne, Uttarakhand 246193, India
[2] The Institute of Mathematical Sciences, C.I.T. Campus, Taramani, Chennai 600113, India
[3] Department of Physics, Hemvati Nandan Bahuguna Garhwal Central University, Srinagar Garhwal, Uttarakhand 246174, India
[4] Centre for Space Research, North-West University, Potchefstroom 2520, South Africa
[5] National Institute for Theoretical and Computational Sciences (NITheCS), Potchefstroom, South Africa
[6] Department of Physics, National Institute of Technology, Agartala, Tripura 799046, India

Received: 21 May 2024 / Accepted: 13 September 2024

Abstract One of the strongest tools to verify the predictions of general relativity (GR) has been the gravitational lensing around various compact objects. Using a dual charged stringy black hole produced from dilaton-Maxwell gravity, we investigate the impact of the plasma parameter on gravitational lensing and black hole shadow in this study. Detailed investigations are performed to mark the impact of the homogeneous and non-homogeneous plasma environment on the electric and magnetic charge parameters of stringy black hole. In order to compare the results, we have also considered the vacuum scenario of the dual charged stringy black hole. Our results show that the effect of homogeneous plasma environment is much stronger in comparison to vacuum for the case of electrically charged stringy black hole. However, in the case of magnetically charged stringy black hole, the deflection angle gets decreased in presence of the homogeneous plasma medium. It has been observed that the radius of the shadow increases in a non-homogeneous plasma environment for electrically charged stringy black hole, whereas it decreases for magnetically charged stringy black hole in presence of the same plasma environment. This study aims to investigate how different plasma environments influence these fascinating astrophysical phenomena.

1 Introduction

Einstein's geometric theory of gravitation, known as General Relativity (GR), has repeatedly passed observational tests in the weak-field domain [1] which makes the GR a widely accepted theory of gravitation. One of the peculiar compact objects predicted by GR in the normal four dimensions (4D) are black holes (BHs), which are essentially the solutions of Einstein's Field Equations (EFEs) in GR [2,3]. The gravitational lensing (GL) is a field that has arisen as one of the consequences of GR and GL hypothesis has been extensively studied in recent years to explain how light moves through a vacuum medium in the vicinity of a compact object [4–11]. In a vacuum, deflection angles depend only on the mass distribution of the lens and not the photon frequency. One of the most potent cosmological techniques, lensing allows for the analysis of the distribution of mass in the cosmos [12,13]. Because light rays in space primarily travel through this medium, it is thus quite interesting to study different aspects of GL in the background of a plasma medium [14].

The nature of a plasma medium is dispersive, i.e., the massless particles (photons) deviate from lightlike geodesics in such a way that only depends on the frequency. The Hamiltonian approach for the photon motion can be derived from Maxwell's approach. In this method, the electromagnetic field source consists of the two charged fluids namely, modelling the ions and the electrons. The transition from Maxwell's equations to ray optics has to be done by a two-scale method by considering a plasma medium on a curved background. Ehlers et al. [15] considered a magnetized pressure-less plasma and provided a stringent derivation approach of the Hamiltonian for light rays. A similar deriva-

[a] e-mail: shubhamkala871@gmail.com
[b] e-mail: hnandan@associates.iucaa.in (corresponding author)
[c] e-mail: Amare.Abebe@nithecs.ac.za
[d] e-mail: sr.phy2011@yahoo.com

Published online: 21 October 2024

tion was obtained by Tsupko et al. for the much simpler case of a non-magnetized pressureless plasma [16]. Further, the equation of photon motion can be characterized by a scalar field, i.e. direction independent, index of refraction which is a function of the spacetime point and of the frequency. Then the resulting equation of motion for massless particles belongs to a specific class that was studied by Synge [17]. The deflection angle of light in the presence of a plasma medium, whose density is a function of the radius coordinate, was calculated in the Schwarzschild BH and Kerr BH by Perlick et al. [18]. The similar outcomes were obtained and addressed in more detail by Bisnovatyi-Kogan and Tsupko [19–21]. Morozova et al. [22] generalized the calculation to the slowly-rotating Kerr BH of the equatorial plane. More recently, the effects of a plasma medium on light rays was studied in greater detail by Er and Mao [23] and Rogers [24]. The effect of GL by a non-Schwarzschild BH and weak GL Schwarzschild-MOG BH in plasma medium is studied by Hakimov and Atamurotov et al. [25,26]. In the weak field approximation of boosted Kerr BH, Bambi et al. [27] studied the effect of light rays in the presence of plasma medium for different distributions viz. singular isothermal sphere, non-singular isothermal gas sphere, and plasma in a galaxy cluster. Further, the behavior of plasma medium on GL of 4D Einstein-Gauss-Bonnet gravity was studied using a distinct method [28]. Furthermore, the influence of plasma medium on weak GL by a naked singularity was investigated by Atamurotov et al. [29]. Recently, the weak GL of a rotating regular BH in a non-minimally coupled Einstein–Yang–Mills (EYM) theory in the presence of plasma medium has been investigated in detail [30]. Several other attempts to investigate the influence of different distribution of plasma medium on GL in various theories of GR and other alternative theories of gravity have also made in recent times. [31–48]

In 2019, the Event Horizon Telescope (EHT) captured the first ever image of the supermassive BH in the galaxy M87* [49–54]. This phenomenon significantly advancing our understanding to explore the mysterious feature of BH physics. The groundbreaking observation of EHT revealed a distinctive structure: a dark central region, known as the BH shadow, surrounded by a luminous ring. The image provides critical insights into the nature of BHs and serves as a crucial test for various theoretical models of their properties. Synge studied the shadow of a spherically symmetric static black hole, specifically in Schwarzschild spacetime, and found that it produced a perfect circular shadow [17]. Later, Bardeen studied the shadow of a rotating black hole and confirmed that it distorts the perfectly circular shape of the shadow [55]. Perlick et al. [56] considered an unspecified spherically symmetric and static spacetime and analytically calculated the influence of a non-magnetized pressure-less plasma on the angular size of the BH shadow. Thereafter, Aatamurotov et al. [57] have studied the shadow and emission rate of axial symmetric rotating Kerr BH in the presence of a plasma with radial power-law density. Furthermore, numerous investigations have been conducted over time to examine whether the presence of plasma around a BH leads to observable effects and references therein [58–63].

The structure of the paper is as follows. We first review the fundamental characteristics of dual charged stringy BH spacetime briefly in Sect. 2. The equation of motion for light-like geodesics in the presence of a plasma medium is then obtained in Sect. 3. In Sect. 4, the exact expressions of the deflection angle for both cases (i.e. electrically and magnetically charged BH) in the presence of homogeneous plasma medium are presented. The deflection angle for the same cases in the presence of nonhomogeneous plasma medium considering the plasma frequency in terms of power law is reported in Sect. 4.1. In Sect. 4.2, the radius of circular orbit is studied for different plasma distributions. The variation of radius of shadow for both the cases in presence of plasma distribution (homogeneous and non-homogeneous) are depicted in Sect. 6. We study the shadow images and density with Infalling Gas in a different plasma distribution in Sect. 6.1 followed by the conclusions drawn out of this study in Sect. 6.2.

2 The dually-charged stringy BH spacetimes

The widely-known asymptotically flat solutions in dilaton-Maxwell gravity which represent BHs with the electric and magnetic charge are due to Garfinkle, Horowitz and Strominger (GHS) [64,65]. The effective action to describe the above solutions in 4D geometry is expressed as,

$$S = \int d^4x\sqrt{-g}\left[-R + 2(\nabla\phi)^2 + e^{-2\phi}F^2\right]. \tag{1}$$

Here $F_{\mu\nu}$ represents the Maxwell field associated with a $U(1)$ subgroup of $E_8 \times E_8$ and ϕ is the dilaton. The dilaton is a scalar field which couples to the Maxwell field. The field equations obtained by extremizing the action with respect to $U(1)$ potential A_μ, ϕ and $g_{\mu\nu}$ are given as follows [64]:

$$\nabla_\mu(e^{-2\phi}F^{\mu\nu}) = 0, \tag{2}$$

$$\nabla^2\phi + \frac{1}{2}e^{-2\phi}F^2 = 0, \tag{3}$$

$$R_{\mu\nu} = 2\nabla_\mu\phi\nabla_\nu\phi + 2e^{-2\phi}F_{\mu\rho}F^\rho_\nu - \frac{1}{2}g_{\mu\nu}e^{-2\phi}F^2. \tag{4}$$

The obtained field equations reduce to standard Einstein scalar field action as in GR by considering $F_{\mu\nu} = 0$. The spacetime geometry arising from the field equations (2–4) have line elements that are causally similar to Schwarzschild geometry in GR as can be observed from the metrics given below. The metric for the BH with electric charge is given as

[66,67]:

$$ds_E^2 = -\frac{\left(1-\frac{m}{r}\right)}{\left(1+\frac{m\sinh^2\alpha}{r}\right)}dt^2 + \frac{dr^2}{\left(1-\frac{m}{r}\right)} + r^2 d\Omega_2^2, \tag{5}$$

where $d\Omega_2^2 = (d\theta^2 + \sin\theta^2 d\phi^2)$ is the metric on a 2D unit sphere and α is a parameter related to the electric charge. The BH with magnetic charge can be obtained from the electrically charged solution using electromagnetic duality transformation [65] and the metric with a magnetic charge parameter is given as follows,

$$ds_M^2 = -\frac{\left(1-\frac{m}{r}\right)}{\left(1-\frac{Q^2}{mr}\right)}dt^2 + \frac{dr^2}{\left(1-\frac{m}{r}\right)\left(1-\frac{Q^2}{mr}\right)} + r^2 d\Omega_2^2. \tag{6}$$

Here, Q is the magnetic charge of the BH. In the respective limits, i.e. $\alpha = 0$ and $Q = 0$, the Schwarzschild BH geometry as in GR can be reproduced directly from both cases as mentioned above.

3 Equation of motion for light rays in plasma medium

Let us consider a generalized spherically symmetric and static metric to obtain the equation of motion for massless particles. The spherically symmetric and static metric is given as,

$$g_{ik}dx^i dx^k = -A(r)dt^2 + B(r)dr^2 + D(r)\left(d\theta^2 + \sin^2\theta d\phi^2\right), \tag{7}$$

where $A(r)$ and $B(r)$ are assumed to be positive in the region outside the event horizon. We are interested in the case of a dually charged stringy BH and for the time being there is no need to specify the metric any further. We consider that the spacetime is filled with a non-magnetized cold and pressureless plasma medium whose electron plasma frequency ω_p is given as a function of the radius coordinate,

$$\omega_p(r)^2 = \frac{4\pi e^2}{m_e}N(r). \tag{8}$$

Here e, m_e and $N(r)$ represent the charge of the electron, the mass of the electron, and the number density of the electrons in the plasma medium, respectively. The refraction index (n) of the plasma medium considered depends on the radial coordinate (r) and the frequency (ω) of the photon as measured by a static observer. Therefore, the refractive index can be expressed as follows,

$$n(r,\omega)^2 = 1 - \frac{\omega_p(r)^2}{\omega^2}. \tag{9}$$

Since the metric is spherically symmetric, each plane can be considered as an equatorial plane so that we may restrict $\theta = \pi/2$, as a result of which $p_\theta = const$ and $\dot{p_\theta} = 0$. Then the Hamiltonian for the motion of light rays in the plasma background reads

$$H = \frac{1}{2}\left[g^{ik}p_i p_k + \omega_p(r)^2\right] = \frac{1}{2}\left[-\frac{p_t^2}{A(r)} + \frac{p_r^2}{B(r)} + \frac{p_\phi^2}{D(r)} + \omega_p(r)^2\right]. \tag{10}$$

The light rays are the solutions to the equations of motion with

$$\dot{p}_i = -\frac{\partial H}{\partial x^i}, \quad \dot{x}^i = \frac{\partial H}{\partial p_i}, \tag{11}$$

which in this case are given as,

$$\dot{p}_t = -\frac{\partial H}{\partial t} = 0, \tag{12}$$

$$\dot{p}_\phi = -\frac{\partial H}{\partial \phi} = 0, \tag{13}$$

$$\dot{p}_r = -\frac{\partial H}{\partial r} = \frac{1}{2}\left[-\frac{p_t^2 A'(r)}{A(r)^2} + \frac{p_r^2 B'(r)}{B(r)^2} + \frac{p_\phi^2 D'(r)}{D(r)^2} - \frac{d}{dr}\omega_p(r)^2\right], \tag{14}$$

$$\dot{t} = \frac{\partial H}{\partial p_t} = -\frac{p_t}{A(r)}, \tag{15}$$

$$\dot{\phi} = \frac{\partial H}{\partial p_\phi} = \frac{p_\phi}{D(r)}, \tag{16}$$

$$\dot{r} = \frac{\partial H}{\partial p_r} = \frac{p_r}{B(r)}, \tag{17}$$

with $H = 0$, i.e.

$$-\frac{p_t^2}{A(r)} + \frac{p_r^2}{B(r)} + \frac{p_\phi^2}{D(r)} + \omega_p(r)^2 = 0. \tag{18}$$

Here, the dot represents differentiation with respect to an affine parameter λ, and a prime denotes differentiation w.r.t r. From Eqs. 12 and 13 it follows that p_t and p_ϕ are constants of motion. Hence, we write $\omega_0 = -p_t$. If we consider the spacetime is asymptotically flat, then first we have to fix the ω_0 and also apply the necessary boundary condition in order to satisfy the spacetime geometry i.e., $A(r) \to 1$ for $r \to \infty$. Therefore, the frequency ω measured by a static observer becomes a function of r by the gravitational redshift formula and yields

$$\omega(r) = \frac{\omega_0}{\sqrt{A(r)}}. \tag{19}$$

The light ray with constant of motion ω_0 is restricted to the region as given in Eq. 18 and satisfied with the following

condition,

$$\frac{\omega_0^2}{A(r)} > \omega_p(r)^2. \tag{20}$$

The physical significance of the condition given in Eq. 20 is that the photon frequency at a given point, $\omega(r)$, must be greater than the frequency of plasma medium, $\omega_p(r)$, at the same point. The propagation of light rays in a plasma medium always satisfies this condition.

The governing equation for the phase trajectory of light can be obtain by using the equation of motion in r and ϕ given by,

$$\frac{dr}{d\phi} = \frac{\dot{r}}{\dot{\phi}} = \frac{D(r)p_r}{B(r)p_\phi}. \tag{21}$$

Substituting the value of p_r in the above equation, we have

$$\frac{dr}{d\phi} = \pm\frac{\sqrt{D(r)}}{\sqrt{B(r)}}\sqrt{\frac{\omega_0^2}{p_\phi^2}h(r)^2 - 1}, \tag{22}$$

where the function $h(r)$ is defined as

$$h(r)^2 = \frac{D(r)}{A(r)}\left[1 - A(r)\frac{\omega_p(r)^2}{\omega_0^2}\right]. \tag{23}$$

4 Deflection angle in presence of homogeneous plasma medium with $\omega_p(r)^2 = constant$

In this section, we consider the gravitational lensing of massless particles in the presence of plasma with i.e., $\omega_p(r)^2 = constant$. The trajectory of orbit must generally be divided into sections where r increases as a function of ϕ and sections where it decreases, as well as the sign in Eq. 22 must be selected properly. Consider a light ray that enters from infinity, decreases to a minimum at radius R, and then expands once again to infinity. With such consideration, the integration over the orbit then leads to the following formula for the bending angle δ:

$$\delta + \pi = 2\int_R^\infty \frac{\sqrt{B(r)}}{\sqrt{D(r)}}\left[\frac{\omega_0^2}{p_\phi^2}h(r)^2 - 1\right]^{-1/2} dr. \tag{24}$$

The turning point of the trajectory corresponds to R so that the condition $dr/d\phi = 0$ must be satisfied. This equation relates R to the constant of motion p_ϕ/ω_0,

$$h(R)^2 = \frac{p_\phi^2}{\omega_0^2}. \tag{25}$$

Then the aforementioned formula for the deflection angle can be expressed as a function of only R and ω_0 (for a given plasma distribution) as follows:

$$\delta + \pi = 2\int_R^\infty \frac{\sqrt{B(r)}}{\sqrt{D(r)}}\left[\frac{h(r)^2}{h(R)^2} - 1\right]^{-1/2} dr. \tag{26}$$

Now, we can obtain the deflection angle for electric and magnetic charged stringy BH, respectively, in the following subsection.

4.1 Case I: stringy BH with electric charge

In this case, we have considered electrically charged spacetime of stringy BH:

$$A(r) = \frac{1 - m/r}{1 + m\sinh^2\alpha/r},$$
$$B(r) = (1 - m/r)^{-1}, \quad D(r) = r^2, \tag{27}$$

with the function $h(r)$ is defined as

$$h(r)^2 = r^2\left[\frac{(r + m\sinh^2\alpha)}{(r - m)} - \frac{\omega_p(r)^2}{\omega_0^2}\right]. \tag{28}$$

Then the bending angle for this case reads

$$\delta_{e(plasma)} = -\pi + 2\int_R^\infty \left[\frac{r^2\left(\frac{(r+m\sinh^2\alpha)}{(r-m)} - \frac{\omega_p(r)^2}{\omega_0^2}\right)}{R^2\left(\frac{(R+m\sinh^2\alpha)}{(R-m)} - \frac{\omega_p(R)^2}{\omega_0^2}\right)} - 1\right]^{-1/2} \times \frac{dr}{\sqrt{r}\sqrt{(r-m)}} \tag{29}$$

The bending angle obtained in Eq. 29 with prescribed limits reduces to electrically charged stringy BH case (for vacuum) and Schwarzschild BH case in GR.

4.2 Case II: stringy BH with magnetic charge

In this case, we have considered a magnetically charged spacetime of stringy BH for which

$$A(r) = \frac{(1 - m/r)}{(1 - Q^2/mr)},$$
$$B(r) = \left[\left(1 - \frac{m}{r}\right)\left(1 - \frac{Q^2}{mr}\right)\right]^{-1}, \quad D(r) = r^2, \tag{30}$$

with the function $h(r)$ defined as

$$h(r)^2 = r^2\left[\frac{rm - Q^2}{(r - m)m} - \frac{\omega_p(r)^2}{\omega_0^2}\right]. \tag{31}$$

Then the bending angle for this case can be expressed as

$$\delta_{m(plasma)} = -\pi + 2\int_R^\infty \left[\frac{r^2\left(\frac{(rm-Q^2)}{(r-m)m} - \frac{\omega_p(r)^2}{\omega_0^2}\right)}{R^2\left(\frac{(Rm-Q^2)}{(R-m)m} - \frac{\omega_p(R)^2}{\omega_0^2}\right)} - 1\right]^{-1/2} \times \frac{dr}{\sqrt{(r-m)}\sqrt{m}\sqrt{rm-Q^2}}. \quad (32)$$

The bending angle obtained in Eq. 32 with prescribed limits reduces to magnetically charged stringy BH case (for vacuum) and the Schwarzschild BH case in GR.

Figure 1 illustrate how the impact parameter b influences the angle of deflection for the dual charge in presence of homogeneous plasma distribution. The top panel of Fig. 1 shows how the deflection angle varies with the impact parameter for various values of the electric charge parameter. As the electric charge rises, we see that the deflection angle approaches its maximum. Further the middle panel of Fig. 1 shows that the variation in deflection is not very substantial for different values of the magnetic charge parameter and that the deflection angle offers the smallest value for the maximum magnetic charge. The behavior of the deflection angle of the dual charged stringy BH and the Schwarzschild BH in the GR in the presence of plasma medium is finally compared in lower panel of Fig. 1. In the presence of plasma, the deflection angle for an electrically charged stringy BH is greater than that of a Schwarzschild BH, whereas for a magnetically charged stringy BH, it is smaller than that of a Schwarzschild BH. The case of dual charged stringy BH is reduced to the vacuum case by the results obtained with the stipulated limit [67].

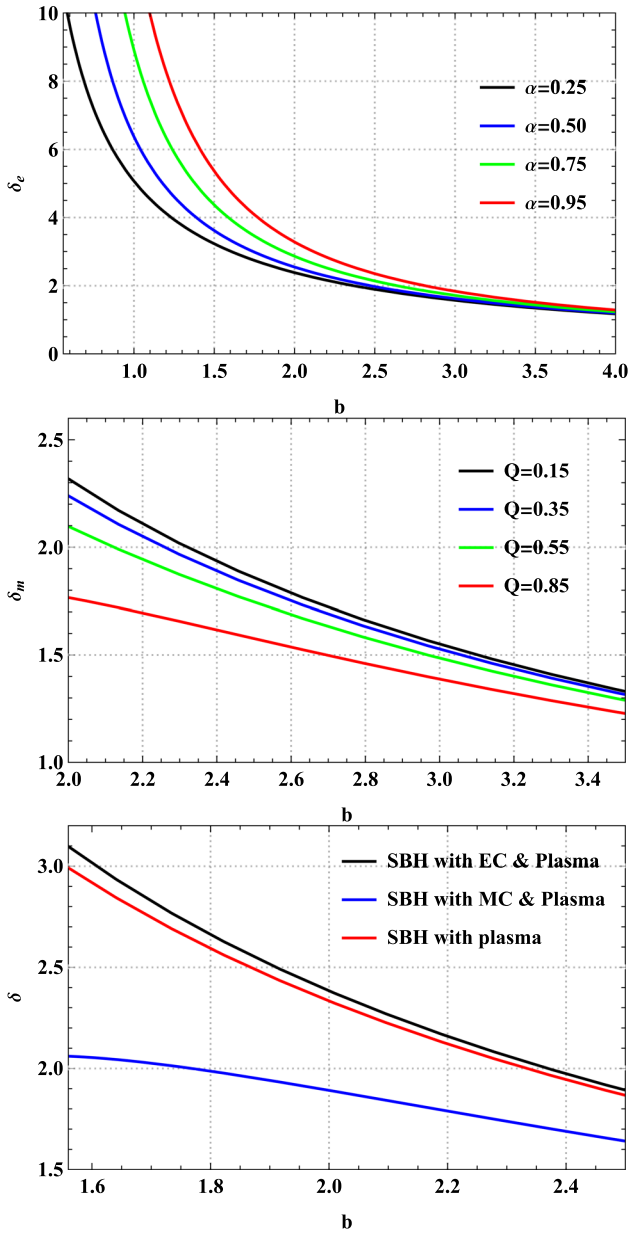

Fig. 1 Deflection angle of dual charged stringy BH with impact parameter for different values of α and Q respectively in homogeneous plasma medium. Here we consider homogeneous plasma parameter is constant i.e, 0.5

5 Deflection angle in presence of non-homogeneous plasma medium with $\omega_p(r)^2 = P_0/r^k$

Now we will obtain the deflection angle in the presence of non-homogeneous plasma, where we consider the plasma frequency in terms of power law form as $\omega_p(r)^2 = P_0/r^k$ [24,68] with $k \geq 0$. Here, P_0 and k are two arbitrary parameters. With $k = 0$, this case will be retreated as the homogeneous case.

5.1 Case I: stringy BH with electric charge

The function $h(r)$ in non homogeneous Plasma medium can be defined as (using Eq. 28)

$$h(r)^2 = r^2\left[\frac{(r + m\sinh^2\alpha)}{(r-m)} - \frac{P_0}{r^k\omega_0^2}\right]. \quad (33)$$

Then the bending angle, by using Eq. 29, for this case can be

$$\delta_{e(plasma)} = -\pi + 2\int_R^\infty \left[\frac{\frac{r^2(r+m\sinh^2\alpha)}{(r-m)} - \frac{P_0}{r^{k-2}\omega_0^2}}{\frac{R^2(R+m\sinh^2\alpha)}{(R-m)} - \frac{P_0}{R^{k-2}\omega_0^2}} - 1\right]^{-1/2} \times \frac{dr}{\sqrt{r}\sqrt{(r-m)}} \quad (34)$$

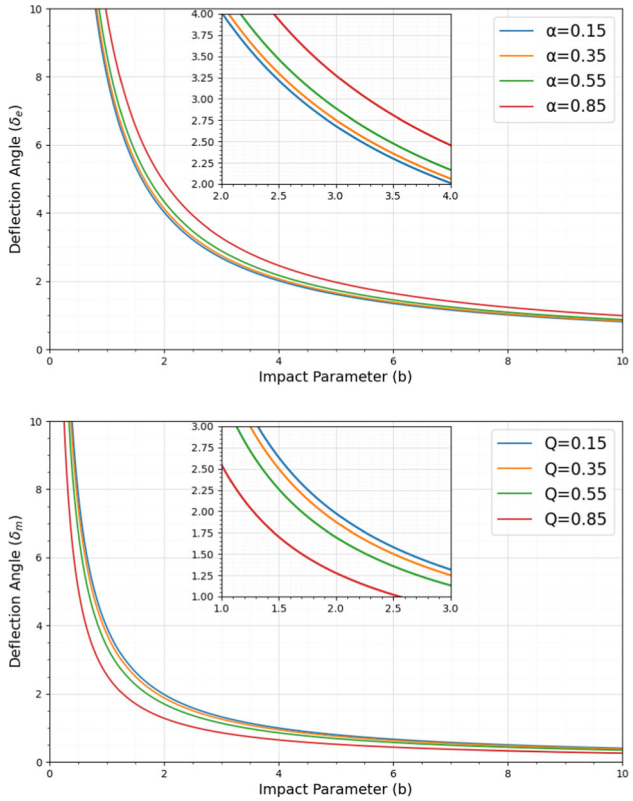

Fig. 2 The variation of bending angle (δ) with impact parameter (b) for different values of electric (upper panel) and magnetic charge (lower panel) parameter. Here we consider $k = 3$ and $\frac{P_0}{\omega_0^2} = 0.5$

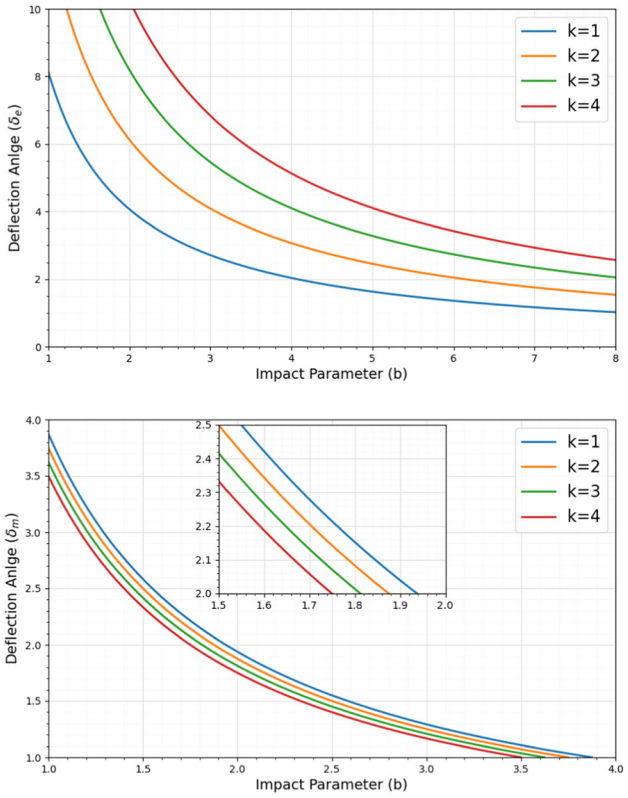

Fig. 3 The variation of bending angle (δ) with impact parameter (b) for different non-homogeneous plasma profiles. Here $\alpha = 0.50$ (upper panel), $Q = 0.50$ (lower panel) and $\frac{P_0}{\omega_0^2} = 0.5$

The bending angle obtained in Eq. 34 for non-homogeneous medium reduces to electrically charged stringy BH.

5.2 Case II: stringy BH with magnetic charge

The function $h(r)$ in non homogeneous Plasma medium is defined as (using Eq. 31)

$$h(r)^2 = r^2\left[\frac{rm - Q^2}{(r-m)m} - \frac{P_0}{r^k\omega_0^2}\right]. \tag{35}$$

Then the bending angle, using Eq. 32, for this case, can be expressed as

$$\delta_{m(plasma)} = -\pi + 2\int_R^\infty \left[\frac{r^2\left(\frac{(rm-Q^2)}{(r-m)m} - \frac{P_0}{r^{k-2}\omega_0^2}\right)}{R^2\left(\frac{(Rm-Q^2)}{(R-m)m} - \frac{P_0}{R^{k-2}\omega_0^2}\right)} - 1\right]^{-1/2} \times \frac{dr}{\sqrt{(r-m)}\sqrt{m}\sqrt{rm-Q^2}}. \tag{36}$$

The bending angle obtained in Eq. 36 for non-homogeneous medium reduces to magnetically charged stringy BH.

The Figs. 2 and 3 express the variation of deflection angle with impact parameter for both electrically and magnetically charged stringy BH in the field of non-homogeneous plasma. Figure 2 depicts that deflection angle increases with the increase of electric charge (α) whereas deflection angle decreases with the increase of magnetic charge (Q). The same characteristics was also observed in Fig. 1 when compared with the Schwarzschild BH in the field of homogeneous plasma. In Fig. 2, we consider $k = 3$ to give the non-homogeneous plasma of $\frac{1}{r^3}$ as the Goldreich-Julian (GJ) density depends on the strength of the polar magnetic field [24]. Figure 3 explains the increase of deflection angle in case of electrically charged stringy BH and decrease of deflection angle in case of magnetically charged stringy BH when we intensify the value of k. Here, $k = 0$ indicates the homogeneous case but Eqs. 34 and 36 show that the deflection due to electrically charged stringy BH and magnetically charged stringy BH would also be same as that of homogeneous plasma for $k = 2$.

6 Circular light orbits

The condition for circular light orbits plays a crucial role for determining the shadow. The condition for a circular light orbit in an unspecified static and spherically symmetric spacetime was first obtained by Atkinson [69]. If we consider a light ray incident tangentially to such a sphere it will stay forever on a circular path with radius r_{ph}. If the spacetime is asymptotically flat, and if $\omega_p(r) \to 0$ for $r \to \infty$, the outermost photon sphere is always unstable with respect to radial perturbations. It indicates that the circular photon orbits in this photon sphere can serve as limit curves for light rays that approach them asymptotically. The radius r_{ph} of the outermost photon sphere is the critical value of the aforementioned minimal radius R. If a light ray comes in from infinity and reaches a minimum radius $R > r_{ph}$, it will go out to infinity again. The condition $R = r_{ph}$ corresponds to a light ray that spirals asymptotically towards a circular photon orbit in the sphere of radius r_{ph}. Further, the remaining rays cross the photon sphere, and we exclude the condition that they can come back. The light rays can come back iff there is a second photon sphere. In this section, we will obtain the condition of circular photon orbit for both cases by using the method of Perlick et al. [56]. The radius of a circular light orbit of light around BH, particularly the one that forms a photon sphere of radius r_{ph} is determined by solving the following equation as,

$$\frac{d}{dr}h(r)^2 = 0. \tag{37}$$

The solution $r = r_{ph}$ to above equation determines the radius of the photon sphere. We can solve this equation by incorporating both homogeneous and nonhomogeneous plasma profiles as described in the previous section. For each plasma profile, the resulting photon radius represents the new radius at which a circular photon orbit exists.

6.1 Case I: stringy BH with electric charge

For the stringy BH with electric charge, where $h(r)$ is given by Eq. 28 as follows;

$$r^2\left[\frac{1}{(r-m)} - \frac{(r+m\sinh^2\alpha)}{(r-m)}\right] + 2r\left[\frac{(r+m\sinh^2\alpha)}{(r-m)} - \frac{\omega_p(r)^2}{\omega_0^2}\right] = 0. \tag{38}$$

Using the condition defined in Eq. 37, one can write the algebraic equation for the radius of a photon sphere in the presence of a plasma medium as

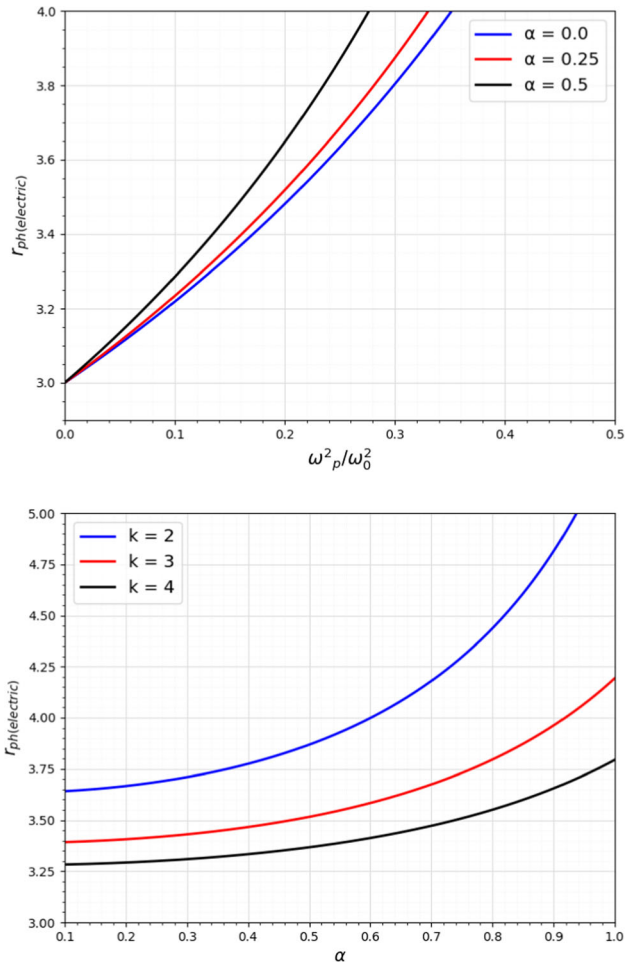

Fig. 4 Radius of photon sphere for electrically charged stringy BH with homogeneous (upper panel) and non-homogeneous (lower panel) plasma medium

$$\frac{r_p\left[2r_p^2 - 2m^2\sinh^2\alpha + mr_p(\sinh^2\alpha - 3)\right]}{(m-r_p)^2} = \frac{2r_p\omega_p(r_p)^2}{\omega_0^2} + \frac{2r_p^2\omega_p(r_p)\omega_p'(r_p)}{\omega_0^2}. \tag{39}$$

6.2 Case II: stringy BH with magnetic charge

For the stringy BH with magnetic charge, where $h(r)$ is given by Eq. 31, condition in Eq. 37 for a photon sphere reads:

$$2r\left[\frac{(rm-Q^2)}{m(r-m)} - \frac{\omega_p(r)^2}{\omega_0^2}\right] - \frac{r^2(rm-Q^2)}{m(r-m)^2} = 0. \tag{40}$$

Using the similar approach, the expression for radius of photon sphere in the presence of plasma medium reads,

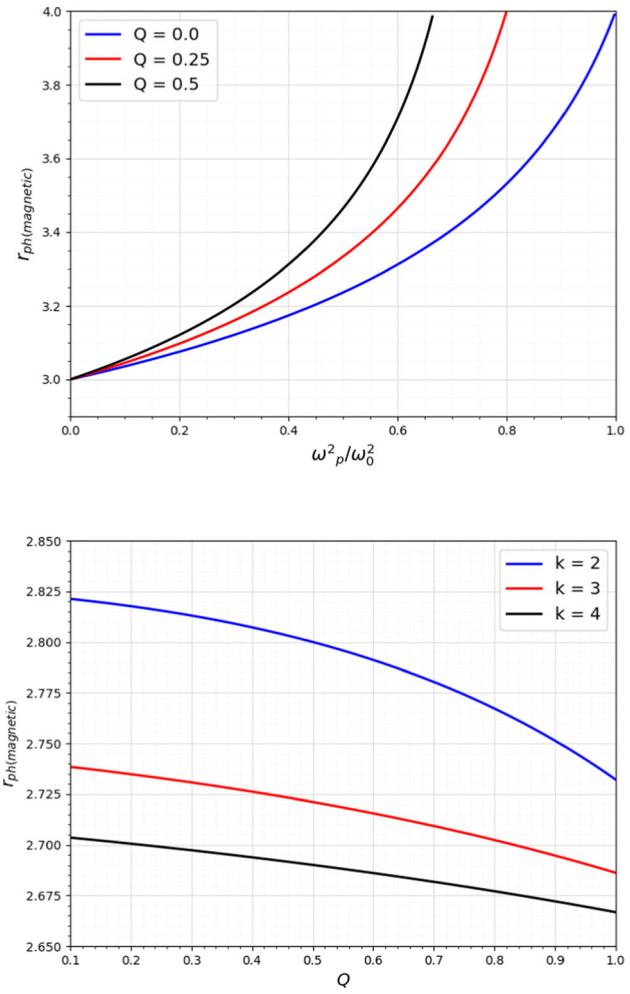

Fig. 5 Radius of photon sphere for magnetically charged stringy BH with homogeneous (upper panel) and non-homogeneous (lower panel) plasma medium

$$\frac{r_p\left[2m(Q^2+r_p^2)-3m^2r_p-Q^2r_p\right]}{m(m-r_p)^2} = \frac{2r_p\omega_p(r_p)^2}{\omega_0^2}+\frac{2r_p^2\omega_p(r_p)\omega_p^{'}(r_p)}{\omega_0^2}. \tag{41}$$

Obviously, the roots of both equations, i.e., Eq. 39 and Eq. 41 cannot be obtained analytically for most variants of $\omega_p(r)$; however, we will consider a few plasma profiles where there exits a circular orbit at every radius for both cases.

The variation of radius of photon sphere of a dual charged stringy BH are depicted in Figs. 4 and 5. We observe that the radius of the photon sphere increases with an increase in the homogeneous plasma parameter for both cases studied. In the presence of a non-homogeneous plasma distribution, the effects of the charges are different: the photon sphere radius increases with an increase in electric charge but decreases with an increase in magnetic charge. This suggests that while a homogeneous plasma uniformly affects the photon sphere radius, a nonhomogeneous plasma introduces charge-dependent variations, where electric and magnetic charges have opposing effects on the radius of the photon sphere.

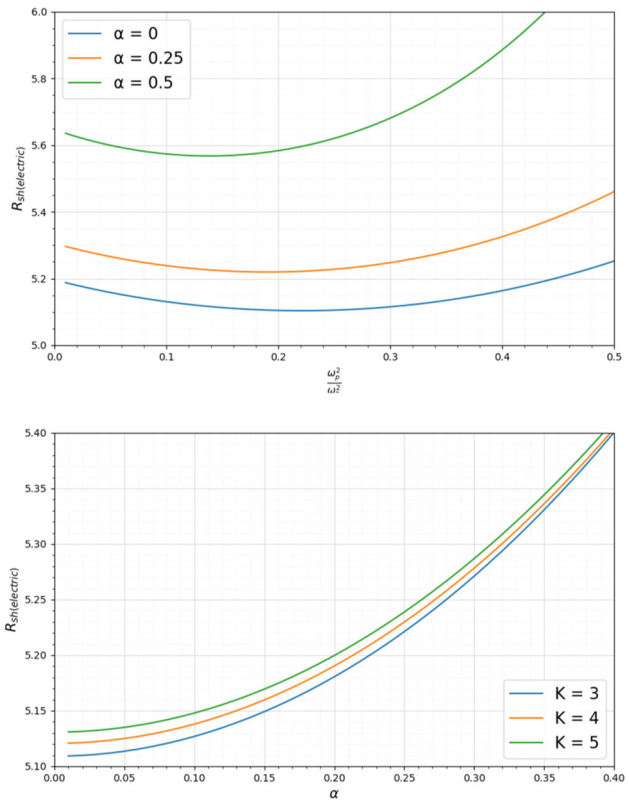

Fig. 6 Shadow's radius of electrically charged stringy BH for homogeneous (upper panel) and non-homogeneous (lower panel) plasma medium

7 Shadow of BH surrounded by plasma medium

In this section, we investigate the radius of shadow of the dual charged stringy BH in the presence of a plasma medium. The angular radius of the BH shadow is defined by geometric approach, which results in the following expression [17,56],

$$\sin^2\alpha_{sh} = \frac{h^2(r_p)}{h^2(r_0)}, \tag{42}$$

where r_0 and r_p represent the locations of the observer and the photon sphere respectively. If the observer is located at a sufficiently large distance from the BH then one can approximate radius of BH shadow as follows,

$$R_{sh} = r_0\sin\alpha_{sh}. \tag{43}$$

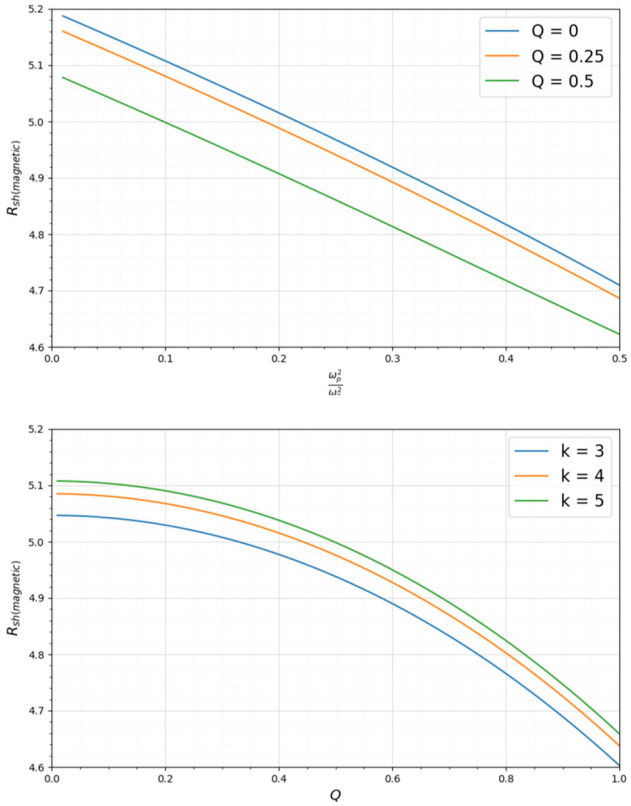

Fig. 7 Shadow's radius of magnetically charged stringy BH for homogeneous (upper panel) and non-homogeneous (lower panel) plasma medium

Case I The radius of the electrically charged stringy BH can be expressed as follows,

$$R_{sh(e)} = \sqrt{r_p^2\left[\frac{(r_p + m\sinh^2\alpha)}{(r_p - m)} - \frac{\omega_p(r_p)^2}{\omega_0^2}\right]}. \tag{44}$$

Case II The radius of the magnetically charged stringy BH can be expressed as follows,

$$R_{sh(m)} = \sqrt{r_p^2\left[\frac{r_p m - Q^2}{(r_p - m)m} - \frac{\omega_p(r_p)^2}{\omega_0^2}\right]}. \tag{45}$$

The obtained results are based on the fact that $h(r) \to r$, which follows from Eq.(23) at spatial infinity for both plasma models. For the vacuum case $\omega_p(r)$, we recover the radius of the dual-charged stringy BH as reported in [67]. Here, we consider the same plasma profile for both homogeneous and nonhomogeneous plasma distributions as described in the previous section.

The variation of shadow radius of a dual charged stringy BH are depicted in Figs. 6 and 7. We observe that the shadow radius decreases with increasing homogeneous plasma parameter in both cases studied. However, for electric charge, the shadow radius initially decreases but slightly increases after reaching a specific plasma parameter value. In the case of non-homogeneous plasma distribution, the effects differ between the two charge types: the shadow radius increases with electric charge and decreases with magnetic charge. Notably, at the same plasma parameter value k (non-homogeneous plasma parameter), the shadow radius exhibits opposite trends for the two types of charge, highlighting a contrasting influence of electric and magnetic charges on the shadow radius under nonhomogeneous plasma conditions.

8 Shadow images with infalling gas in a plasma medium

Here, we consider a simple model of optically thin radiating accretion flow around the dual charged stringy BH in presence of plasma medium. For emission mechanisms, certain assumptions shall be made for the calculation of the intensity from the radiating accretion flow. The observed specific intensity $I_{\nu 0}$ at the observed photon frequency $\nu_{\rm obs}$ at the point (X, Y) of the observer's image (usually measured in ergs^{-1}cm^{-2}str^{-1}Hz^{-1}) is given by [70],

$$I_{obs}(\nu_{obs}, X, Y) = \int_\gamma g^3 j(\nu_e) dl_{\rm prop}, \tag{46}$$

where $g = \nu_{obs}/\nu_e$ is the redshift factor, ν_e is the photon frequency as measured in the rest-frame of the emitter, $j(\nu_e)$ is the emissivity per unit volume in the rest-frame of the emitter, and $dl_{\rm prop} = k_\rho u_e^\rho d\lambda$ is the infinitesimal proper length as measured in the rest-frame of the emitter. The redshift fucntion g can be calculated by the relation,

$$g = \frac{k_\rho u^\rho_{\rm obs}}{k_\sigma u_e^\sigma}, \tag{47}$$

where k^μ is the 4-velocity of the photons, u_e^ρ 4-velocity of the accreting gas emitting the radiation and $u^\mu_{\rm obs}$ is 4-velocity of the observer with λ is the affine parameter along the photon path γ.

The whole integral given by Eq. (42) should be evaluated over the path γ of the photons i.e. (null geodesics). In order to generalise the formalism for both the cases, we will restrict to the equatorial plane only and assume that the gas is radially free falling with a four-velocity whose components are described below,

$$\begin{aligned} u_e^t &= \frac{1}{g_{tt}(r)}, \\ u_e^r &= -\sqrt{\frac{1 - g_{tt}(r)}{g_{tt}(r)g_{rr}(r)}}, \\ u_e^\theta &= 0, \\ u_e^\phi &= 0, \end{aligned} \tag{48}$$

where the metric components g_{tt}, g_{rr} and $g_{\phi\phi}$ are corresponding to the line elements for Case I and Case II. In previous

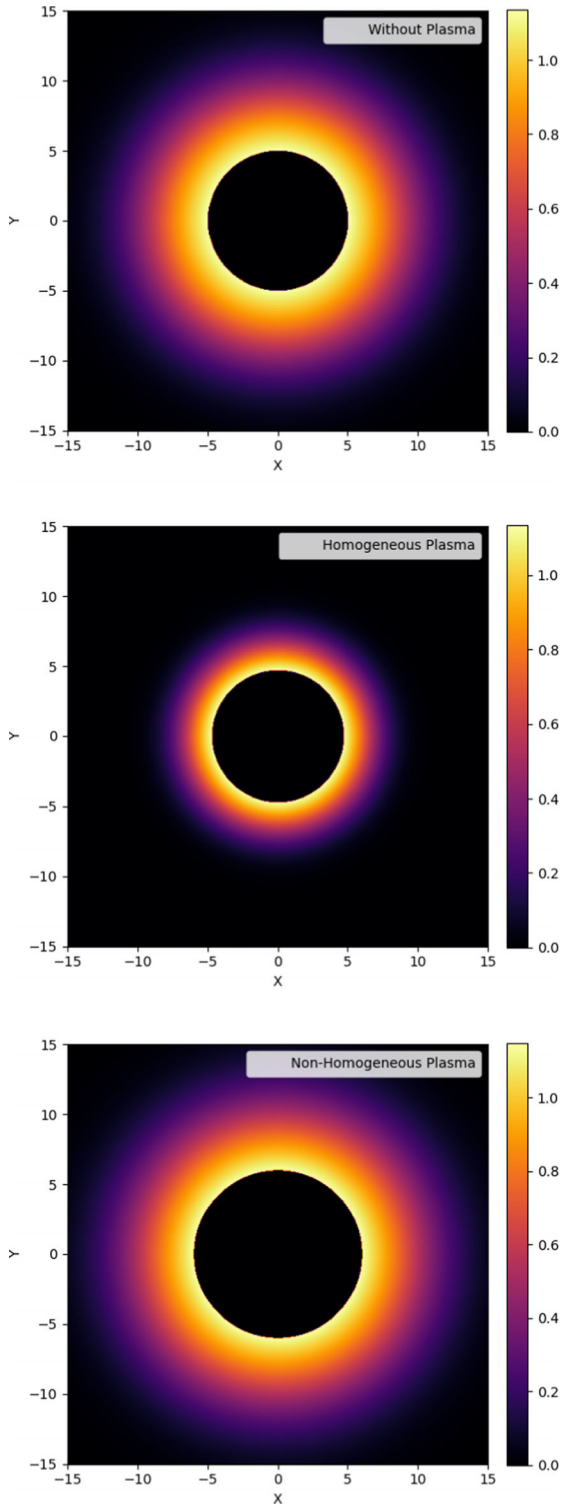

Fig. 8 Shadow images for a electric charged stringy BH with and without plasma medium. Here we have set $\frac{\omega_p(r)^2}{\omega_0^2} = 0.50$ (homogeneous) and $k = 3$ (non-homogeneous) and $\alpha = 0.50$. X and Y represents the angular celestial coordinates in the observer's sky

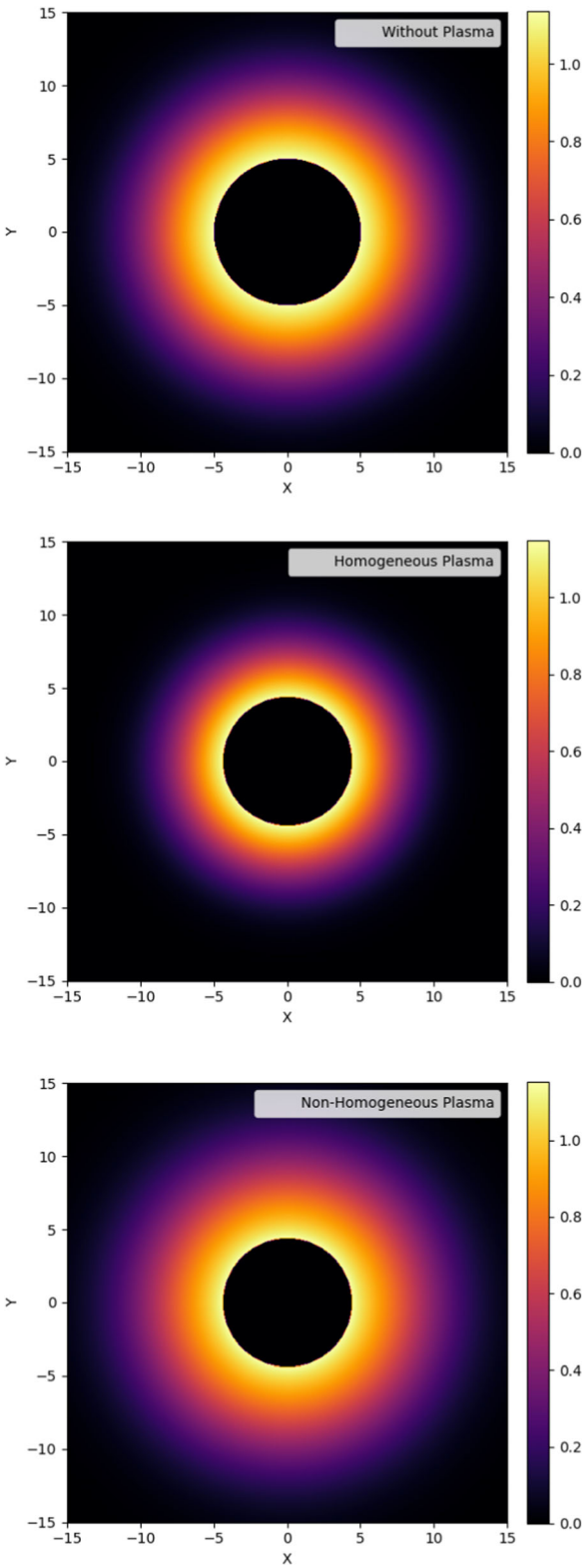

Fig. 9 Shadow images for a magnetic charged stringy BH with and without plasma medium. Here we have set $\frac{\omega_p(r)^2}{\omega_0^2} = 0.50$ (homogeneous) and $k = 3$ (non-homogeneous) and $Q = 0.50$. X and Y represents the angular celestial coordinates in the observer's sky

section, the components of four-velocity were already calculated. In order to ease further calculations, we obtain an equation between the radial and time component of the four-velocity as follows,

$$\frac{k_r}{k_t} = \pm\sqrt{g_{rr}\left(\frac{1}{g_{tt}} - \frac{b^2}{g_{\phi\phi}}\right)}, \tag{49}$$

where the sign $+(-)$ corresponds to photon approaches (goes away) from the massive object. The redshift function g is then given by,

$$g = \frac{1}{\frac{1}{g_{tt}} \pm \frac{k_r}{k_t}\sqrt{\left(\frac{1-g_{tt}}{g_{tt}g_{rr}}\right)}}. \tag{50}$$

The specific emissivity for a simple model in which the emission is monochromatic with emitter's-rest frame frequency $\nu_\star$, and the emission has a $1/r^2$ radial profile is calculated as,

$$j(\nu_e) \propto \frac{\delta_D(\nu_e - \nu_\star)}{r^2}, \tag{51}$$

where δ_D is the Dirac delta function. The proper length can be written as,

$$dl_{\text{prop}} = k_\rho u_e^\rho d\lambda = -\frac{k_t}{g|k^r|}dr, \tag{52}$$

Integrating the Intensity over all the observed frequencies, we obtain the observed photon intensity as given below,

$$I_{obs}(X, Y) \propto -\int_\gamma \frac{g^3 k_t}{r^2 k^r}dr. \tag{53}$$

Now we have the desired intensity equation so we can proceed to compute the images. We closely follow the numerical technique presented in [71,72] and modified for the use of stringy BH spacetimes as Case I and Case II accordingly. The shadow images and intensities of the dual charged stringy BH for vacuum, homogeneous and non-homogeneous medium are depicted in Figs. 8 and 9 respectively. In case of electrically charged stringy BH, we observe that the shadow and intensities decrease in homogeneous plasma medium but both are increases in non-homogeneous plasma medium. However, in a different scenario we observed for magnetically charged stringy BH. Compared to the case of vacuum, the shadow radius decreases for both homogeneous as well as non-homogeneous plasma medium. Further, the density decreases in homogeneous plasma medium but increases in non-homogeneous plasma medium. We thus found that, the presence of plasma distribution significantly affect the observational characteristics of a BH, such as the shadow size and intensity.

9 Summary, conclusion and future directions

In this paper, we have studied the deflection angle and black hole shadow of a dual charged stringy BH immersed in a homogeneous and non-homogeneous plasma medium. We consider the plasma frequency in terms of power law to examine the previously mentioned astrophysical effect in a nonhomogeneous plasma environment. First, we have analysed the motion of a photon around this BH spacetime in brief. Using the Hamilton-Jacobi formalism, we have obtained the equations of motion and the deflection angle of light around both stringy BH spacetimes in the presence of a plasma medium. Further, we studied the BH shadow radius and shadow images considering the Infalling Gas in a plasma environment. The results obtained for both plasma environment can be summarized as follows:

Homogeneous plasma medium

The analysis of the deflection of light ray around a dual-charged stringy BH in the plasma medium shows that the effect of the plasma environment is much stronger in comparison to vacuum for the case of electrically charged (α) stringy BH. However, in the case of magnetically charged (Q) stringy BH the deflection angle is decreasing in the presence of the plasma medium. We have also obtained the necessary condition of circular bound orbits for both cases. We observe that the radius of the photon sphere increases with an increase in the homogeneous plasma parameter for both cases studied. We observe that the shadow radius decreases with increasing homogeneous plasma parameter in both cases studied. However, for electric charge, the shadow radius initially decreases but slightly increases after reaching a specific plasma parameter value. In case of electrically charged stringy BH, we observe that the shadow intensities decrease in homogeneous plasma medium, but a different scenario we observed for magnetically charged stringy BH.

Non-homogeneous plasma medium

The analysis of the deflection angle in a non-homogeneous plasma environment shows that the deflection angle increases with increasing electric charge (α) whereas the deflection angle decreases with the increase of magnetic charge (Q). The same characteristics were also observed in the Schwarzschild BH in the field of homogeneous plasma. We also found the increase of deflection angle in case of electrically charged stringy BH and decrease of deflection angle in case of magnetically charged stringy BH when we intensify the value of nonhomogeneous plasma parameter. In particular, the value of $k = 0$ indicates the homogeneous case, but

Eqs. 34 and 36 show that the deflection due to electrically charged stringy BH and magnetically charged stringy BH would also be the same as that of homogeneous plasma for $k = 2$.

Future directions

We plan to study the effect of different plasma profiles on the lensing and shadow of charged, rotating and accelerating BHs in the future. Since it is well known that for a rotating case the shape of the BH shadow remains no longer circular, the proposed study may thus provide valuable information about the effect of the plasma parameter on the shape and size of BH shadows.

Acknowledgements The authors express sincere gratitude to the anonymous referee for their invaluable feedback and insights, which greatly contributed to the improvement of this manuscript. Their detailed and thoughtful review was instrumental in enhancing the quality of this work. The authors S.K. and H.N. acknowledge the use of facilities at ICARD, Gurukula Kangri (Deemed to be University), Haridwar, India. One of the authors, H.N., would also like to thank IUCAA, Pune, for the support under its associateship program where a part of this work was done. The author HN also acknowledges the financial support provided by the Science and Engineering Research Board (SERB), New Delhi, through Grant number CRG/2023/008980.

Data Availability Statement This manuscript has no associated data. [Author's' comment: Data sharing not applicable to this article as no datasets were generated or analysed during the current study.]

Code Availability Statement This manuscript has no associated code/software. [Author's comment: Code/Software sharing not applicable to this article as no code/software was generated or analysed during the current study.]

Funded by SCOAP[3].

References

1. J.B. Hartle, *Gravity: An Introduction to Einstein's General Relativity* (Cambridge University Press, Cambridge, 2003)
2. P.S. Joshi, Int. Ser. Monogr. Phys. **87**, 87 (1993)
3. S. Chandrasekhar, *The Mathematical Theory of Black Holes*, vol. 69 (Oxford University Press, Oxford, 1998)
4. B. Paczynski, Astrophys. J. **304**, 1 (1986). https://doi.org/10.1086/164140
5. K.S. Virbhadra, G.F.R. Ellis, Phys. Rev. D **62**, 084003 (2000). https://doi.org/10.1103/PhysRevD.62.084003
6. V. Bozza, S. Capozziello, G. Iovane, G. Scarpetta, Gen. Relativ. Gravit. **33**, 1535 (2001). https://doi.org/10.1023/A:1012292927358
7. V. Bozza, Phys. Rev. D **66**, 103001 (2002). https://doi.org/10.1103/PhysRevD.66.103001
8. V. Bozza, L. Mancini, Astrophys. J. **611**, 1045 (2004). https://doi.org/10.1086/422309
9. V. Bozza, L. Mancini, Astrophys. J. **627**, 790 (2005). https://doi.org/10.1086/430664
10. V. Bozza, G. Scarpetta, Phys. Rev. D **76**, 083008 (2007). https://doi.org/10.1103/PhysRevD.76.083008
11. V. Bozza, Gen. Relativ. Gravit. **42**, 2269 (2010). https://doi.org/10.1007/s10714-010-0988-2
12. M. Bartelmann, P. Schneider, Phys. Rep. **340**, 291 (2001). https://doi.org/10.1016/S0370-1573(00)00082-X
13. T. Treu, Ann. Rev. Astron. Astrophys. **48**, 87 (2010). https://doi.org/10.1146/annurev-astro-081309-130924
14. J. Neufeld, R.H. Ritchie, Phys. Rev. **98**, 1632 (1955). https://doi.org/10.1103/Phys.Rev.98.1632
15. J. Ehlers, A.R. Prasanna, R.A. Breuer, Class. Quantum Gravity **4**, 253 (1987). https://doi.org/10.1088/0264-9381/4/2/009
16. O.Y. Tsupko, G. Bisnovatyi-Kogan, Gravit. Cosmol. **18**(2), 117 (2012)
17. J.L. Synge, Mon. Not. R. Astron. Soc. **131**(3), 463 (1966). https://doi.org/10.1093/mnras/131.3.463
18. V. Perlick, O.Y. Tsupko, Phys. Rev. D **95**(10), 104003 (2017). https://doi.org/10.1103/Phys.Rev.D.95.104003
19. O.Y. Tsupko, G.S. Bisnovatyi-Kogan, Gravit. Cosmol. **15**, 184 (2009). https://doi.org/10.1134/S0202289309020182
20. G.S. Bisnovatyi-Kogan, O.Y. Tsupko, Mon. Not. R. Astron. Soc. **404**, 1790 (2010). https://doi.org/10.1111/j.1365-2966.2010.16290.x
21. O.Y. Tsupko, G.S. Bisnovatyi-Kogan, Phys. Rev. D **87**(12), 124009 (2013). https://doi.org/10.1103/Phys.Rev.D.87.124009
22. V. Morozova, B. Ahmedov, A. Tursunov, Astrophys. Space Sci. **346**, 513–523 (2013)
23. X. Er, S. Mao, Mon. Not. R. Astron. Soc. **437**(3), 2180 (2014). https://doi.org/10.1093/mnras/stt2043
24. A. Rogers, Mon. Not. R. Astron. Soc. **451**(1), 17 (2015)
25. A. Hakimov, F. Atamurotov, Astrophys. Space Sci. **361**(3), 1 (2016)
26. F. Atamurotov, A. Abdujabbarov, J. Rayimbaev, Eur. Phys. J. C **81**(2), 1 (2021)
27. C.A. Benavides-Gallego, A.A. Abdujabbarov, C. Bambi, Eur. Phys. J. C **78**(9), 694 (2018). https://doi.org/10.1140/epjc/s10052-018-6170-9
28. G.Z. Babar, F. Atamurotov, A.Z. Babar, Phys. Dark. Univ. **32**, 100798 (2021). https://doi.org/10.1016/j.dark.2021.100798
29. F. Atamurotov, S.G. Ghosh, Eur. Phys. J. Plus **137**(6), 662 (2022). https://doi.org/10.1140/epjp/s13360-022-02885-3
30. S. Kala, H. Nandan, P. Sharma, Eur. Phys. J. Plus **137**(4), 457 (2022). https://doi.org/10.1140/epjp/s13360-022-02634-6
31. G.S. Bisnovatyi-Kogan, O.Y. Tsupko, Plasma Phys. Rep. **41**, 562 (2015). https://doi.org/10.1134/S1063780X15070016
32. F. Atamurotov, F. Sarikulov, V. Khamidov, A. Abdujabbarov, Eur. Phys. J. Plus **137**(5), 567 (2022). https://doi.org/10.1140/epjp/s13360-022-02780-x
33. F. Atamurotov, F. Sarikulov, A. Abdujabbarov, B. Ahmedov, Eur. Phys. J. Plus **137**(3), 336 (2022). https://doi.org/10.1140/epjp/s13360-022-02548-3
34. F. Atamurotov, A. Abdujabbarov, W.B. Han, Phys. Rev. D. **104**(8), 084015 (2021). https://doi.org/10.1103/Phys.Rev.D.104.084015

35. X.H. Jin, Y.X. Gao, D.J. Liu, Int. J. Mod. Phys. D **29**(09), 2050065 (2020). https://doi.org/10.1142/S0218271820500650
36. F. Atamurotov, K. Jusufi, M. Jamil, A. Abdujabbarov, M. Azreg-Aïnou, Phys. Rev. D **104**(6), 064053 (2021). https://doi.org/10.1103/Phys.Rev.D.104.064053
37. G. Crisnejo, E. Gallo, K. Jusufi, Phys. Rev. D **100**(10), 104045 (2019). https://doi.org/10.1103/Phys.Rev.D.100.104045
38. G.Z. Babar, F. Atamurotov, S. Ul Islam, S.G. Ghosh, Phys. Rev. D **103**(8), 084057 (2021). https://doi.org/10.1103/Phys.Rev.D.103.084057
39. V. Perlick, O.Y. Tsupko, Phys. Rev. D **109**(6), 064063 (2024). https://doi.org/10.1103/PhysRevD.109.064063
40. A. Davlataliev, B. Narzilloev, I. Hussain, A. Abdujabbarov, B. Ahmedov, Phys. Dark Univ. **42**, 101340 (2023). https://doi.org/10.1016/j.dark.2023.101340
41. S. Kumar, A. Uniyal, S. Chakrabarti, Phys. Rev. D **109**(10), 104012(2024). https://doi.org/10.1103/PhysRevD.109.104012
42. S. Orzuev, F. Atamurotov, A. Abdujabbarov, A. Abduvokhidov, New Astron. **105**, 102104 (2024). https://doi.org/10.1016/j.newast.2023.102104
43. F. Atamurotov, O. Yunusov, A. Abdujabbarov, G. Mustafa, New Astron. **105**, 102098 (2024). https://doi.org/10.1016/j.newast.2023.102098
44. F. Atamurotov, H. Alibekov, A. Abdujabbarov, G. Mustafa, M.M. Aripov, Symmetry **15**(4), 848 (2023). https://doi.org/10.3390/sym15040848
45. Q. Li, Y. Zhang, Z.W. Lin, Q.Q. Li, Q. Sun, Mod. Phys. Lett. A **38**(04), 2350025 (2023). https://doi.org/10.1142/S0217732323500256
46. A. Ditta, T. Xia, M. Yasir, Int. J. Mod. Phys. A **38**(06n07), 2350041 (2023). https://doi.org/10.1142/S0217751X23500410
47. N.U. Molla, U. Debnath, Ann. Phys. **453**, 169304 (2023). https://doi.org/10.1016/j.aop.2023.169304
48. W. Javed, S. Riaz, R.C. Pantig, A. Övgün, Eur. Phys. J. C **82**(11), 1057 (2022). https://doi.org/10.1140/epjc/s10052-022-11030-4
49. K. Akiyama et al., Astrophys. J. **875**(1), L1 (2019). https://doi.org/10.3847/2041-8213/ab0ec7
50. K. Akiyama et al., Astrophys. J. Lett. **875**(1), L2 (2019). https://doi.org/10.3847/2041-8213/ab0c96
51. K. Akiyama et al., Astrophys. J. Lett. **875**(1), L3 (2019). https://doi.org/10.3847/2041-8213/ab0c57
52. K. Akiyama et al., Astrophys. J. Lett. **875**(1), L4 (2019). https://doi.org/10.3847/2041-8213/ab0e85
53. K. Akiyama et al., Astrophys. J. Lett. **875**(1), L5 (2019). https://doi.org/10.3847/2041-8213/ab0f43
54. K. Akiyama et al., Astrophys. J. Lett. **875**(1), L6 (2019). https://doi.org/10.3847/2041-8213/ab1141
55. J. Bardeen, Black holes, in ed. c. Dewitt, B.S. Dewitt Proceedings, Ecole d'Eté de Physique Théorique: Les Astres Occlus : Les Houches, France, August, 197, pp. 215–240 (1973)
56. V. Perlick, O.Y. Tsupko, G.S. Bisnovatyi-Kogan, Phys. Rev. D **92**(10), 104031 (2015). https://doi.org/10.1103/Phys.Rev.D.92.104031
57. F. Atamurotov, B. Ahmedov, A. Abdujabbarov, Phys. Rev. D **92**(8), 084005 (2015)
58. Y. Huang, Y.P. Dong, D.J. Liu, Int. J. Mod. Phys. D **27**(12), 1850114 (2018). https://doi.org/10.1142/S0218271818501146
59. S.K. Jha, S. Aziz, A. Rahaman, Eur. Phys. J. C **82**(2), 106 (2022). https://doi.org/10.1140/epjc/s10052-022-10042-4
60. J. Badía, E.F. Eiroa, Phys. Rev. D **107**(12), 124028 (2023). https://doi.org/10.1103/PhysRevD.107.124028
61. G. Briozzo, E. Gallo, T. Mädler, Phys. Rev. D **107**(12), 124004 (2023). https://doi.org/10.1103/PhysRevD.107.124004
62. F. Atamurotov, M. Jamil, K. Jusufi, Chin. Phys. C **47**(3), 035106 (2023). https://doi.org/10.1088/1674-1137/acaef7
63. M.A. Raza, M. Zubair, E. Maqsood, JCAP **05**, 047 (2024). https://doi.org/10.1088/1475-7516/2024/05/047
64. D. Garfinkle, G.T. Horowitz, A. Strominger, Phys. Rev. D **43**, 3140 (1991). https://doi.org/10.1103/Phys.Rev.D.43.3140, https://doi.org/10.1103/Phys.Rev.D.45.3888. [Erratum: Phys. Rev. D. 45, 3888 (1992)]
65. D. Garfinkle, G.T. Horowitz, A. Strominger Phys. Rev. D **43**, 3140 (1991). https://doi.org/10.1103/PhysRevD.43.3140 [Erratum: Phys.Rev.D 45, 3888 (1992)]
66. A. Dasgupta, H. Nandan, S. Kar, Phys. Rev. D **79**, 124004 (2009). https://doi.org/10.1103/Phys.Rev.D.79.124004
67. S. Kala, Saurabh, H. Nandan, P. Sharma, Int. J. Mod. Phys. A **35**(28), 2050177 (2020). https://doi.org/10.1142/S0217751X20501778
68. X. Er, A. Rogers, Mon. Not. R. Astron. Soc. **475**(1), 867 (2018)
69. R.D. Atkinson, Astron. J. **70**, 517 (1965)
70. M. Jaroszynski, A. Kurpiewski, Astron. Astrophys. **326**, 419 (1997)
71. K. Saurabh, K. Jusufi, Eur. Phys. J. C **81**(6), 490 (2021). https://doi.org/10.1140/epjc/s10052-021-09280-9
72. K. Jusufi, Saurabh, Mon. Not. R. Astron. Soc. **503**(1), 1310 (2021)